

Nodeless superconductivity in the SnAs-based van der Waals type superconductor NaSn_2As_2

E. J. CHENG,¹ J. M. NI,¹ F. Q. MENG,² T. P. YING,¹ B. L. PAN,¹ Y. Y. HUANG,¹ DARREN PEETS,¹ Q. H. ZHANG,² AND S. Y. LI^{1,3,*(a)}

¹ State Key Laboratory of Surface Physics, Department of Physics, and Laboratory of Advanced Materials, Fudan University, Shanghai 200433, China

² Beijing National Laboratory for Condensed Matter Physics, Institute of Physics, Chinese Academy of Sciences, School of Physical Sciences, University of Chinese Academy of Sciences, Beijing 100190, China

³ Collaborative Innovation Center of Advanced Microstructures, Nanjing 210093, China

PACS 74.25.Bt – Thermodynamic properties
 PACS 74.25.F – Transport properties
 PACS 74.25.-q – Properties of superconductors

Abstract – We grew the single crystals of the SnAs-based van der Waals (vdW)-type superconductor NaSn_2As_2 and systematically measured its resistivity, specific heat, and ultralow-temperature thermal conductivity. The superconducting transition temperature $T_c = 1.60$ K of our single crystal is 0.3 K higher than that previously reported. A weak but intrinsic anomaly situated at 193 K is observed in both resistivity and specific heat, which likely arises from a charge-density-wave (CDW) instability. Ultralow-temperature thermal conductivity measurements reveal a fully-gapped superconducting state with a negligible residual linear term in zero magnetic field, and the field dependence of κ_0/T further suggests NaSn_2As_2 is an s -wave superconductor.

Introduction. – Phonon-mediated conventional superconductors possess s -wave pairing symmetry, while unconventional ones prefer d -wave, p -wave or s_{\pm} -wave and their pairing glues are likely not phonon [1]. Unconventional superconductivity usually resides in quasi-two-dimensional (quasi-2D) compounds, such as cuprates, iron-based superconductors, Sr_2RuO_4 , heavy-fermion and organic superconductors [2–6]. In the field of condensed-matter physics, one of the most intriguing themes is finding new quasi-2D superconductors and illuminating their underlying superconducting pairing mechanism.

Quasi-2D superconductors with weak vdW force in interlayers can be exfoliated into monolayer or few atomic-layers films [7]. By mechanically reducing the dimensionality of a vdW-type superconductor, it is possible to realize a highly crystalline 2D superconducting system with exotic property that differs from the bulk [8–10]. For example, Ising superconductivity and a field-induced Bose-metal phase were observed in atomically-thin NbSe_2 [9, 10]. Moreover, with the development of ionic gating techniques, the superconducting transition temperature

can be tuned [11]. To explore more exotic phenomena and clarify the superconducting pairing mechanism in the vdW-type superconductors, different types of compounds are highly desirable.

Recently, the first superconducting 2D SnAs-based compound, NaSn_2As_2 with a bulk $T_c = 1.3$ K, was reported [12]. Later, its sister compound $\text{Na}_{1-x}\text{Sn}_2\text{P}_2$ with $T_c = 2.0$ K was also discovered [13]. As schematically shown in Fig. 1(a), NaSn_2As_2 consists of SnAs bilayers separated by Na^+ cations crystallizing a trigonal $R\bar{3}m$ unit cell, which is structurally different from the tetragonal “122” iron-based superconductors [3]. NaSn_2As_2 can be exfoliated into monolayer or few-layers films by using liquid-phase or mechanical lift-off techniques, making it a vdW-type superconductor [8, 14]. Stoichiometric, NaSn_2As_2 is a non-electron-balanced compound assuming a +2 oxidation state for Sn, and -3 oxidation state for As [12]. In NaSn_2As_2 , the Sn^{2+} ions are accompanied by lone-pair electrons [12]. Lone-pair electrons lead to a strong anharmonicity because of the nonlinear terms in the total energy relevant to a large nonhybrid valence electronic contribution, resulting in low thermal conductivity as well as structural distortion [15]. This is reminiscent of

^(a)E-mail: shiyan.li@fudan.edu.cn

the RE(O,F)BiS₂ compounds (RE represents rare earth elements) which includes Bi³⁺ lone pair electrons, and the lone-pair effect is likely relevant to superconductivity [17]. Recent literature also reported on unconventional superconducting pairing mechanism in RE(O,F)BiS₂ compounds [18], which contrasts with previous study [16]. This inspires us to explore the superconducting pairing symmetry of NaSn₂As₂ with lone-pair electrons.

In this paper, we present the growth of high-quality NaSn₂As₂ single crystals, and systematic measurements of their resistivity, specific heat, and ultralow-temperature thermal conductivity. The $T_c = 1.60$ K of our single crystals is 0.3 K higher than that in Ref. [12]. A previously unobserved anomaly around 193 K is evidenced from both resistivity and specific heat, with its origin may closely related to the formation of CDW. Ultralow-temperature thermal conductivity measurements demonstrate that NaSn₂As₂ is an *s*-wave superconductor with a nodeless superconducting gap.

Experiments. – Single crystalline NaSn₂As₂ was synthesized by a Sn-flux method, which is different from that of previous reports [12, 14]. Arsenic lumps (99.999%, Aladdin), sodium chunks (99.99%, Aladdin), and tin powder (99.999%, Aladdin) in the ratio Na : Sn : As = 1 : 10 : 2 were used as starting materials. A charge of 1.0 g was put in an alumina crucible and sealed in a quartz ampoule. The sealed ampoule was heated to 750 °C and kept there for 3 days, then cooled at a rate of 1.5 K/h. The ampoule was taken out and decanted with a centrifuge to remove excess Sn flux at 350 °C, acquiring plate-like single crystals, as shown in the left inset in Fig. 1(c).

For transport measurements, the NaSn₂As₂ single crystal was cleaved and cut into a rectangular shape of dimensions 3.0 × 0.5 mm² in the *ab* plane, with 0.2 mm thickness along the *c* axis. Four electrodes were directly attached on the sample surface with silver paint, and the typical contact resistance is 30 mΩ at 0.3 K. Resistivity measurements from 300 to 2 K and down to 0.3 K were performed in a physical property measurement system (PPMS; Quantum Design) and a ³He cryostat, respectively. Heat capacity measurements were conducted using the relaxation method in a PPMS equipped with a dilution refrigerator. Microstructure analysis was performed on Tecnai F20 and H-9000NA transmission electron microscopes both equipped with low-temperature holders. The thermal conductivity study was conducted in a dilution refrigerator via a standard four-wire steady-state method with two RuO₂ chip thermometers calibrated *in situ* against a reference RuO₂ thermometer. Magnetic fields were normal to the *ab* plane and the heat current. To obtain a homogeneous field distribution in the NaSn₂As₂ single crystal, magnetic fields were applied at a temperature above T_c for both resistivity and thermal conductivity measurements.

Results and discussion. – From x-ray diffraction measurements, as shown in Fig. 1(c), the largest surface

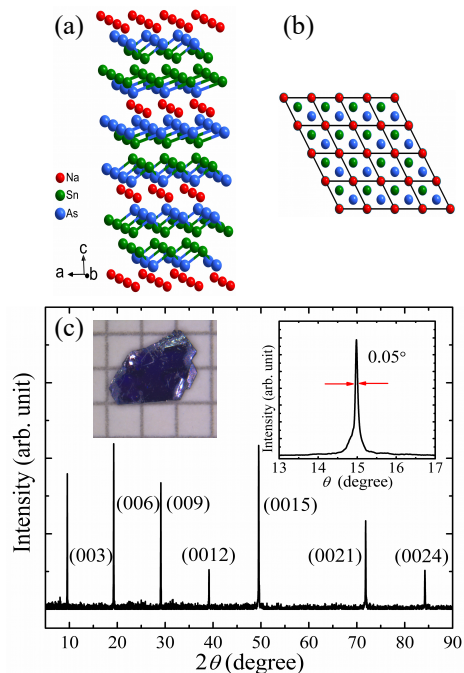


Fig. 1: (a) Crystal structure of NaSn₂As₂. Red, green and blue spheres represent Na, Sn and As, respectively. (b) The view of the NaSn₂As₂ crystal structure down the *c* axis. (c) X-ray diffraction pattern of the NaSn₂As₂ single crystal. Left inset: optical image of a typical NaSn₂As₂ single crystal placed on grid paper with one grid unit 1 × 1 mm². Right inset: X-ray rocking curve of (009) Bragg peak having a full width at half maximum of 0.05°.

of the single crystals is identified to be the (00*l*) plane of NaSn₂As₂. From an X-ray rocking curve of the (009) Bragg peak, the full width at half maximum (FWHM) of 0.05° indicates the high quality of the NaSn₂As₂ single crystal. In Fig. 2(a), we present the resistivity of a NaSn₂As₂ single crystal from 0.3 to 300 K. The resistivity curve from 2 to 10 K is fitted by adopting the formula $\rho = \rho_0 + AT^n$, obtaining a residual resistivity $\rho_0 = 60.3 \mu\Omega$ cm and $n = 3.5$. The residual resistivity ratio (RRR) $\rho(300 \text{ K})/\rho_0$ of 3.7 is larger than the 1.6 reported in [12], manifesting better sample quality.

In addition to the superconducting transition at low temperature in Fig. 2(a), there are two eye-catching features at the normal state that are worth pointing out and may imply rich physics. The first of all, the fitting factor of the lower region is 3.5 (as shown in the upper inset of Fig. 2(a)), which is higher than the T^2 of Fermi-liquid behavior but lower than the T^5 relation caused by phonon scattering. According to the notion proposed by A. H. Wilson, scattering from a low-mass band into a high-density one could induce a higher power law of temperature than that predicted by Fermi-liquid theory in resistivity [19]. And the plausible scattering mechanism can be charge-density or spin-density fluctuation.

The second prominent feature is a kink situated at 193

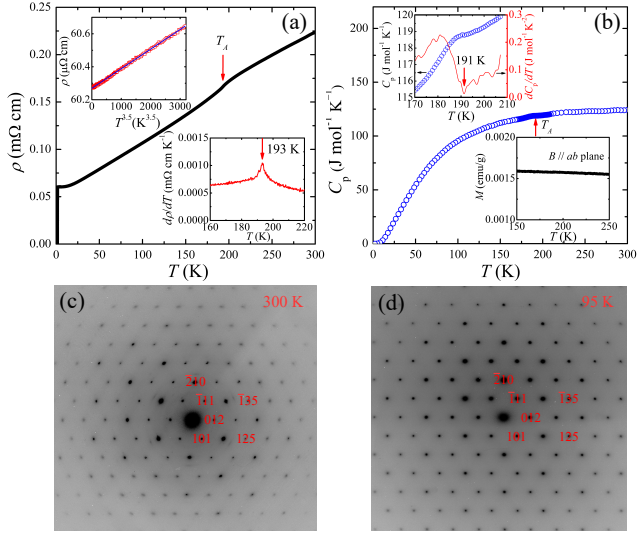


Fig. 2: (a) Low-temperature resistivity of NaSn_2As_2 single crystal from 0.3 to 300 K; the weak anomaly at 193 K is marked as T_A . The inset in the upper left demonstrates the low-temperature power law by plotting ρ vs T^n , with $n = 3.5$. Right inset shows the derivative of resistivity with respect to temperature together across the kink at 193 K. (b) Specific heat of a NaSn_2As_2 single crystal. A weak phase transition at 191 K is shown and marked with a red arrow. The left inset shows the phase transition and the derivative of the specific heat with respect to temperature. The right inset displays the susceptibility result with a magnetic field of 0.5 T. (c) and (d) show the electron diffraction patterns of NaSn_2As_2 at 300 and 95 K, respectively.

K, which has not been reported before [12]. This anomaly is in consistent with our specific heat experiment where a weak peak around 191 K is observed, as shown in Fig. 2 (b). Notwithstanding the weak signal, we incline to think this kink is intrinsic, if considering the high quality of our single crystals and the bulk sensitive of the specific heat measurement. Contrast to the sharp “ λ ”-shape peak associated with structural phase transition, this broad peak should not originate from a first-order structural phase transition. In order to further verify that the anomaly is not rooted in a structural phase transition, we carried out the room- and low-temperature electron diffraction experiments. Figure 2(c) displays the diffraction pattern of NaSn_2As_2 at 300 K, which can be indexed to a hexagonal unit cell which agrees well with the crystalline structure of NaSn_2As_2 . Typical diffraction spots, such as (101), (012), $(\bar{1}11)$, $(\bar{2}10)$, $(\bar{1}35)$, and (125), can be well indexed. Below the anomaly temperature, the diffraction pattern of 95 K is almost identical to that of 300 K, excluding a structural phase transition.

To check if the anomaly arises from a magnetic phase transition, the susceptibility measurement was conducted. As shown in the inset of Fig. 2(b), no anomaly around 193 K appears. Recent electronic structure calculations

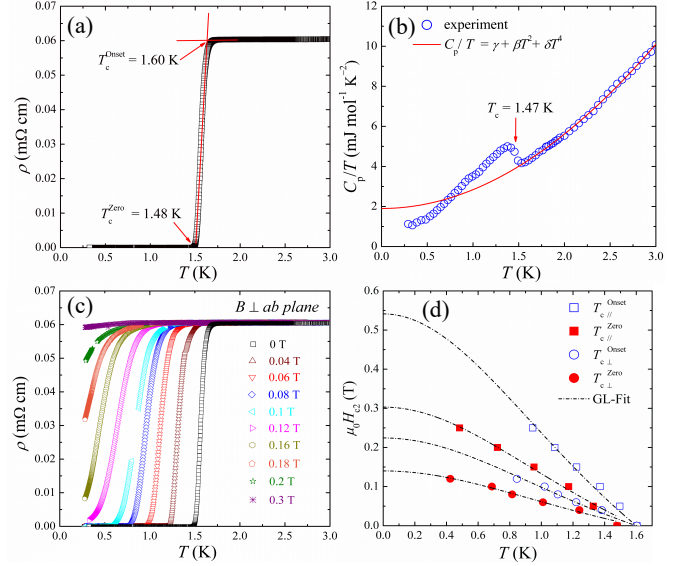


Fig. 3: (a) Low-temperature resistivity of NaSn_2As_2 single crystal in zero field. The T_c is defined as the intersection of two straight lines, which gives 1.60 K and 1.48 K for onset and zero-point T_{cs} , respectively. (b) Temperature dependence of specific heat divided by temperature at low temperature. The red line shows the fitting above the superconducting state with $C_p/T = \gamma + \beta T^2 + \delta T^4$. (c) Low-temperature resistivity at magnetic fields perpendicular to the ab plane. (d) The upper critical fields defined by onset and zero-point superconducting temperatures with field perpendicular and parallel to the ab plane.

on NaSn_2As_2 found that its electronic states near fermi level (E_F) are primarily derived from the contribution of nonmagnetic Sn- s , Sn- p , and some As- p orbitals [14], which further suggests that this compound lies far from magnetic instabilities. CDWs often appear in 2D compounds [21], and are accompanied by superlattice [21,22]. Together with a weak broad peak in specific heat and a higher power law of temperature in resistivity, we speculate that the anomaly in 2D NaSn_2As_2 might arise from a CDW instability. The failed observation of a superlattice pattern at low temperature should be due to the weakness of the CDW in NaSn_2As_2 . To verify this speculation, more solid evidence will be required.

The superconducting transition in the resistivity is plotted in Fig. 3(a), and the T_{cs} are 1.60 and 1.48 K for the onset and zero-point (T_c^{Onset} , T_c^{Zero}) temperatures, respectively. Figure 3(b) shows the low-temperature specific heat divided by the temperature, C_p/T , as a function of temperature in zero field. The superconducting transition at 1.47 K corresponds to the observation in resistivity. Above T_c , the data from 1.5 to 3 K of C_p/T vs T can be well fitted by $C_p/T = \gamma + \beta T^2 + \delta T^4$. The electronic specific heat coefficient γ and the phononic coefficient β are determined to be $1.90 \text{ mJ mol}^{-1} \text{ K}^{-2}$ and $0.94 \text{ mJ mol}^{-1} \text{ K}^{-4}$, respectively. The Debye temperature $\Theta_D \approx 218 \text{ K}$ is estimated by adopting the formula

$\Theta_D = (12\pi^4 r N_A k_B / 5\beta)^{1/3}$, where $r = 5$ is the number of atoms per formula unit, N_A is the Avogadro constant, and k_B is the Boltzmann constant, respectively. Figure 3(c) plots the low-temperature resistivity of NaSn_2As_2 in various magnetic fields up to 0.3 T showing that the superconducting transition is gradually suppressed with magnetic field. Considering the Ginzburg-Landau theory, $\mu_0 H_{c2}(T) = \mu_0 H_{c2}(0) (1-t^2)/(1+t^2)$, here $t = T/T_c$, the zero-temperature upper critical field $\mu_0 H_{c2}(0)$ is estimated. As shown in Fig. 3(d), the upper critical fields H_{c2s} defined by the onset and zero-point temperatures ($T_{c\perp}^{\text{Onset}}$ and $T_{c\perp}^{\text{Zero}}$) are 0.22 and 0.14 T, respectively, for magnetic fields normal to the ab plane. The H_{c2s} with field parallel to the ab plane are also yielded, and the values give 0.54 and 0.30 T for onset and zero-point temperatures, respectively. Based on these values of H_{c2s} , the superconducting state of quasi-2D NaSn_2As_2 is anisotropic.

Ultralow-temperature thermal conductivity measurement is an established bulk technique to probe the superconducting gap structure [23]. In unconventional superconductors, symmetry-imposed nodes are often observed within the superconducting gap [23]. In our experiment, thermal conductivity can be separated into two contributions, κ_e and κ_p , associated with the one from electrons and phonons, respectively. In order to study their specific contributions, the formula $\kappa/T = a + bT^{\alpha-1}$ [23] is adopted for fitting, with the two terms aT and bT^{α} represent contributions from electrons and phonons, respectively. The residual linear term κ_0/T of $-1 \pm 1 \mu\text{W K}^{-2} \text{cm}^{-1}$ is obtained by extrapolating the κ/T to zero temperature (See Fig. 4(a)). Noting that a negative κ_0/T intercept is unphysical, the value of κ_0/T is negligible with our experimental error bar of $\pm 5 \mu\text{W K}^{-2} \text{cm}^{-1}$.

As for the parameter of α , its value is typically between 2 and 3 because of specular reflections of phonons at the sample surfaces [23]. For s -wave nodeless superconductors, there are no fermionic quasiparticles to conduct heat as $T \rightarrow 0$, since all electrons become Cooper pairs [23]. Therefore, there is no residual linear term of κ_0/T , as seen in Nb, InBi and NbSe_2 [24–26]. However, for nodal superconductors, a substantial κ_0/T in zero field contributed by the nodal quasiparticles has been found. For example, κ_0/T of the overdoped ($T_c = 15$ K) d -wave cuprate superconductor $\text{Tl}_2\text{Ba}_2\text{CuO}_{6+\delta}$ (Tl-2201) is $1.41 \text{ mW K}^{-2} \text{cm}^{-1}$, $\sim 36\% \kappa_{N0}/T$ [27]. For the p -wave superconductor Sr_2RuO_4 ($T_c = 1.5$ K), $\kappa_0/T = 17 \text{ mW K}^{-2} \text{cm}^{-1}$ was reported, more than $9\% \kappa_{N0}/T$ [4]. Hence, the negligible κ_0/T of NaSn_2As_2 strongly suggests a nodeless superconducting gap structure.

Figure 4(b) shows κ/T vs T plots of temperature-dependent thermal conductivity for a NaSn_2As_2 single crystal under magnetic fields. All the data of κ/T vs T are fitted and the κ_0/T for each field is obtained. In 0.12 T and 0.14 T, the value of κ_0/T is 0.43 ± 0.04 and $0.42 \pm 0.04 \text{ mW K}^{-2} \text{cm}^{-1}$, respectively. We determined the normal-state expectation value of the Wiedemann-Franz law L_0/ρ_0 (0.12 T) = $0.41 \text{ mW K}^{-2} \text{cm}^{-1}$, where the

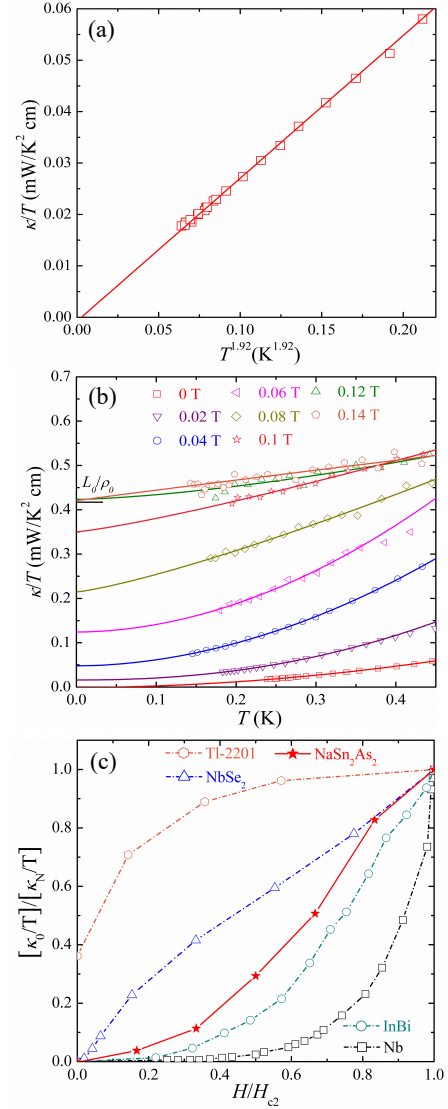


Fig. 4: (a) Low-temperature thermal conductivity of NaSn_2As_2 single crystal in zero field and (b) magnetic fields. The solid lines in both zero field and fields represent the fitting according to the formula of $\kappa/T = a + bT^{\alpha-1}$. In zero field, the value of the residual linear term κ_0/T is $-1 \pm 1 \mu\text{W} / \text{K}^2 \text{cm}$, which is negligible. In an applied field at 0.12 T, κ_0/T meets the normal-state Wiedemann-Franz law expectation L_0/ρ_0 . (c) Normalized residual linear term κ_0/T of NaSn_2As_2 as a function of H/H_{c2} , with bulk $H_{c2} = 0.12$ T. Data on the clean s -wave superconductor Nb [24], the dirty s -wave superconductor InBi [25], the multiband s -wave superconductor NbSe_2 [26], and the overdoped d -wave cuprate superconductor Tl-2201 [27] are included for comparison.

Lorenz number $L_0 = 2.45 \times 10^{-8} \text{ W } \Omega \text{ K}^{-2}$ and ρ_0 (0.12 T) = $60.3 \mu\Omega \text{ cm}$. The value of κ_0/T in 0.12 T meets the expectation, which means that the normal state has been reached. Note that the H_{c2} defined by $\rho = 0$ is 0.14 T, when magnetic field perpendicular to the ab plane. Therefore, the upper critical fields of NaSn_2As_2 in our thermal conductivity and resistivity experiments are con-

sistent, which demonstrates that our thermal conductivity measurements are reliable.

Further information on the superconducting pairing symmetry can be provided by examining the behavior of field-dependent $\kappa_0(H)/T$ as a function of H/H_{c2} [28], as shown in Fig. 4(c). Data on the clean s -wave superconductor Nb [24], the dirty s -wave superconductor InBi [25], the multiband s -wave superconductor NbSe₂ [26], and the overdoped d -wave cuprate superconductor Tl-2201 [27] are plotted for comparison. For the single-band clean s -wave superconductor Nb, $\kappa_0(H)/T$ grows exponentially with field [24], while for the s -wave InBi in the dirty limit, the curve is exponential at low H and displays roughly linear behavior closer to H_{c2} [25]. For nodal superconductor Tl-2201, a small field can yield a quick growth due to the Volovik effect, and the low-field $\kappa_0(H)/T$ shows a roughly \sqrt{H} dependence [27]. In the case of NbSe₂, the distinct $\kappa_0(H)/T$ behavior was well explained by multiple superconducting gaps with different magnitudes [26].

By comparing the curve of the normalized $\kappa_0(H)/T$ for NaSn₂As₂ with others, the field dependence of $\kappa_0(H)/T$ most closely resembles that of InBi. The faster growth has two possible explanations. One is that NaSn₂As₂ is a multiple-band superconductor. However, from ARPES experiments, there is only a hole-type band crossing E_F , and hole carriers dominate the density of states of the Fermi surface at low temperature [14]. Therefore, we exclude this explanation. The other possibility is that NaSn₂As₂ is a “dirty” superconductor. However, due to the lack of Fermi velocity in NaSn₂As₂, we can not derive the electron mean free path l . Thus, it is an open question whether NaSn₂As₂ is an s -wave superconductor in the dirty limit.

Summary. – In summary, we synthesized NaSn₂As₂ single crystals using a Sn-flux method, and a superconducting transition temperature $T_c = 1.60$ K is found. From ultralow-temperature thermal conductivity experiments, a fully-gapped superconducting state has been revealed. The field dependence of κ_0/T further confirms that NaSn₂As₂ is an s -wave superconductor. A weak anomaly at 193 K is discovered, and we propose that the anomaly might arise from a CDW instability. Further work is needed to determine whether the anomaly results from a CDW instability, and illuminate the interplay between CDW and superconductivity with lone-pair electrons.

This work is supported by the Ministry of Science and Technology of China (Grant No. 2015CB921401 and 2016YFA0300503), the Natural Science Foundation of China (Grant No. 11422429 and 11421404), and the NSAF (Grant No. U1630248).

REFERENCES

- [1] NORMAN M. R., *Science*, **332** (2011) 196.
- [2] LEE P. A., NAGAOSA N., AND WEN X. G., *Rev. Mod. Phys.*, **78** (2006) 17.
- [3] CHEN X. H., DAI P. C., FENG D. L., XIANG T. AND ZHANG F. C., *Natl. Sci. Rev.*, **1** (2014) 371.
- [4] MACKENZIE A. P. AND MAENO Y., *Rev. Mod. Phys.*, **75** (2003) 657.
- [5] PFLEIDERER C., *Rev. Mod. Phys.*, **81** (2009) 1551.
- [6] SINGLETON J., *Rep. Prog. Phys.*, **63** (2000) 1111.
- [7] NOVOSELOV K. S., MISHCHENKO A., CARVALHO A., CASTRO NETO A. H., *Science*, **353** (2016) 6298.
- [8] KIM J. S., *JPSJ News and Comments*, **14** (2017) 13.
- [9] XI X., WANG Z., ZHAO W., PARK J. H., LAW K. T., BERGER H., FORRÓ L., SHAN J., AND MAK K. F., *Nat. Phys.*, **12** (2016) 139.
- [10] TSEN A. W., HUNT B., KIM Y. D., YUAN Z. J., JIA S., CAVA R. J., HONE J., KIM P., DEAN C. R., AND PASUPATHY A. N., *Nat. Phys.*, **12** (2016) 208.
- [11] XI X. X., BERGER H., FORRÓ L., SHAN J., AND MAK K. F., *Phys. Rev. Lett.*, **117** (2016) 106801.
- [12] GOTO Y., YAMADA A., MATSUDA T. D., AOKI Y. AND MIZUGUCHI Y., *J. Phys. Soc. Jpn.*, **86** (2017) 123701.
- [13] GOTO Y., AKIRA MIURA, MORIYOSHI C., KUROIWA Y., MATSUDA T. D., AOKI Y., AND MIZUGUCHI Y., *arXiv:1805.07847*, (2018) .
- [14] ARGUILLA M. Q., KATOCH J., KRYMOWSKI K., CULTRARA N. D., XU J., XI X., HANKS A., JIANG S., ROSS R. D., KOCH R. J., ULSTRUP S., BOSTWICK A., JOZWIAK C., MCCOMB D. W., ROTENBERG E., SHAN J., WINDL W., KAWAKAMI R. K. AND GOLDBERGER J. E., *ACS Nano*, **10** (2016) 9500.
- [15] NIELSEN M. D., OZOLINS V., AND HEREMANS J. P., *Environ. Environ. Sci.*, **6** (2013) 570.
- [16] YAMASHITA T., TOKIWA Y., TERAZAWA D., NAGAO M., WATAUCHI S., TANAKA I., TERASHIMA T., AND MATSUDA Y., *J. Phys. Soc. Jpn.*, **85** (2016) 073707.
- [17] MIZUGUCHI Y., PARIS E., SUGIMOTO T., IADECOLA A., KAJITANI J., MIURA O., MIZOKAWA T., AND SAINI N. L., *Phys. Chem. Chem. Phys.*, **17** (2015) 22090.
- [18] OTA Y., OKAZAKI K., YAMAMOTO H. Q., YAMAMOTO T., WATANABE S., CHEN C. T., NAGAO M., WATAUCHI S., TANAKA I., TAKANO Y., AND SHIN S., *Phys. Rev. Lett.*, **118** (2017) 167002.
- [19] WILSON A. H., *Proc. R. Soc. A*, **167** (1938) 580.
- [20] KUSMARTSEVA A. F., SIPOS B., BERGER H., FORRÓ L., AND TUTIŠ E., *Phys. Rev. Lett.*, **103** (2009) 236401.
- [21] GABOVICH A. M., VOITENKO A. I., AUSLOOS M., *Phys. Rep.*, **367** (2002) 583.
- [22] GRNER G., *Rev. Mod. Phys.*, **60** (1988) 1129.
- [23] SHAKERIPOUR H., PETROVIC C. AND TAILLEFER L., *New J. Phys.*, **11** (2009) 055065.
- [24] LOWELL J. AND SOUSA J. B., *J. Low. Temp. Phys.*, **3** (1970) 65.
- [25] WILLIS J. O. AND GINSBERG D. M., *Phys. Rev. B*, **14** (1976) 1916.
- [26] BOAKNIN E., TANATAR M. A., PAGLIONE J., HAWTHORN D., RONNING F., HILL R. W., SUTHERLAND M., TAILLEFER L., SONIER J., HAYDEN S. M. AND BRILL J. W., *Phys. Rev. Lett.*, **90** (2003) 117003.
- [27] PROUST C., BOAKNIN E., HILL R. W., TAILLEFER L.,

- AND MACKENZIE A. P., *Phys. Rev. Lett.*, **89** (2002) 147003.
[28] LI S. Y., TAILLEFER L., WU G., AND CHEN X. H., *Phys. Rev. Lett.*, **99** (2007) 107001.